Effective interactions and nuclear structure using 180 MeV protons. I. $^{16}O(p,p')$

J. J. Kelly,[a] J. M. Finn,[b] W. Bertozzi,[c] T. N. Buti,[d] F. W. Hersman,[e] C. Hyde-Wright,[f] M. V. Hynes,[g] M. A. Kovash,[h] B. Murdock,[i] P. Ulmer,[b] A. D. Bacher,[j] G. T. Emery,[k] C. C. Foster,[j] W. P. Jones,[j] D. W. Miller,[j] and B. L. Berman[l]

[a]*University of Maryland, College Park, Maryland 20742*
[b]*College of William and Mary, Williamsburg, Virginia 23185*
[c]*Massachusetts Institute of Technology, Cambridge, Massachusetts 02139*
[d]*IBM Corporation, Hopewell Junction, New York 12533*
[e]*University of New Hampshire, Durham, New Hampshire 03824*
[f]*University of Washington, Seattle, Washington 98195*
[g]*Los Alamos National Laboratory, Los Alamos, New Mexico 87545*
[h]*University of Kentucky, Lexington, Kentucky 40506*
[i]*Tektronics, Inc., Beaverton, Oregon 97077*
[j]*Indiana University, Bloomington, Indiana 47405*
[k]*Bowdoin College, Brunswick, Maine 04011*
[l]*George Washington University, Washington, DC 20052*

(Received 27 November 1989)

Differential cross sections and analyzing powers for scattering of 180 MeV protons by ^{16}O have been measured for all narrow states below 12.1 MeV of excitation. Medium modifications to the effective interaction for normal-parity isoscalar transitions were studied using transition densities determined by electron scattering to minimize nuclear structure uncertainties. An empirical effective interaction, guided by nuclear matter theory, was fitted to inelastic scattering data for six states simultaneously. Distorted waves were generated from self-consistent optical potentials computed from the same effective interaction. The isoscalar effective interaction determined by this procedure provides a good global fit to the inelastic scattering data and is consistent with elastic scattering data that were not included in the fit. The results are consistent with earlier results for 135 MeV and show that the effective interaction is suppressed at low density but is less density dependent than predicted by nuclear matter theory and the local density approximation. These comparisons suggest effects in finite nuclei beyond the local density approximation. Finally, we compare data for 0^- and 2^- states at both 135 and 180 MeV with representative calculations.

I. INTRODUCTION

The complementary aspects of electron scattering and proton scattering can be exploited to considerable advantage in a combined analysis of data for the same set of nuclear transitions excited by either probe. For isoscalar normal-parity transitions in self-conjugate targets, electroexcitation measurements of transition charge densities almost completely determine the nuclear structure information required to interpret complementary proton scattering data. The two-nucleon effective interaction is then isolated for study with little residual uncertainty due to nuclear structure. Empirical medium modifications can be fitted to inelastic scattering data and compared with nuclear matter theory. Then, armed with an accurate effective interaction, neutron transition densities can be extracted from proton scattering data for nearby isotopes provided that the corresponding proton transition densities are available from electron scattering data. Therefore, combined analyses of electron and proton scattering data promise to yield considerable insight into effective interactions and nuclear structure.

In this the first in a series of three papers discussing proton scattering data at 180 MeV, we present new data for ^{16}O and study the effective interaction using the methods of Refs. 1 and 2. In particular, we fit an empirical effective interaction to inelastic scattering data for six states simultaneously and compare the results to the nuclear matter predictions of Refs. 3–5. The essential characteristics of the empirical effective interaction are the same as previously found at 135 MeV,[1] namely, that the low-density interaction is suppressed and the density dependence reduced with respect to expectations based upon the local density approximation (LDA) and nuclear matter theory. In the second paper[6] we use new data for ^{28}Si to study the possible dependence of the effective interaction upon target. We find that a unique effective interaction describes both data sets consistently. Finally, in the third paper[7] we use existing (e,e') data and new $^{30}Si(p,p')$ data to study neutron transition densities.

The experiment is described in Sec. II and the reaction model in Sec. III. Our results for normal-parity transitions are presented in Secs. IV A and IV B and for abnormal parity in Sec. IV C. Finally, our conclusions are discussed in Sec. V.

II. EXPERIMENT

The experiment was performed using 179.9 MeV protons at the Indiana University Cyclotron Facility. Scat-

 ©1990 The American Physical Society

tered protons were analyzed by the dispersion matched QDDM spectrometer and detected with a standard focal plane array consisting of a helical wire chamber and two plastic scintillators. The relative efficiency was found constant within 0.4%, which was added in quadrature to cross-section uncertainties. The beam current was measured with an external Faraday cup, believed accurate to about 1%, for angles $\theta \geq 24°$. A smaller Faraday cup within the scattering chamber was used for $\theta \leq 24°$. The relative normalization between internal and external cups was found to be 0.919 ± 0.015.

Several beryllium oxide (BeO) wafers, with thicknesses between 22 and 290 mg/cm^2, were used as targets. A 26.76 mg/cm^2 pure ^{9}Be target was used to obtain data for broad states in ^{9}Be and to constrain the background. Cross sections measured with several targets agreed within ±5%, which we estimate to be the systematic uncertainty in normalization.

The beam polarization was measured approximately every eight hours using the low-energy ^{4}He polarimeter located after the injector cyclotron. The polarization was typically 0.80 for spin-up and 0.75 for spin-down and varied little between measurements. Additional uncertainties of ±0.008 for spin-up and ±0.020 for spin-down were added in quadrature to the measured beam polarizations to account for fluctuations between measurements.

The offset in scattering angle was determined by comparing elastic scattering measurements performed on either side of the beam. From the cross-section measurements we found $\Delta\theta = 0.013° \pm 0.005°$ needed to be added to the spectrometer angle. The offset resulting from the analyzing power measurements turned out to be somewhat larger, namely, $\Delta\theta = 0.09° \pm 0.03°$. However, the latter measurement is vulnerable to false asymmetries due to alignment errors or to sideways polarization components. Therefore, we omit $\Delta\theta$ from the data tables and claim knowledge of the scattering angle better than 0.1°.

A typical spectrum, with about 100 keV resolution FWHM, is shown in Fig. 1. The spectrum was fitted using the ALLFIT program described in Refs. 2 and 8. Intrinsic widths of 25 keV for the 4_1^+ state at 10.353 MeV and 70 keV for the 2_3^+ state at 11.521 MeV were included by convoluting Lorentzian line shapes with the intrinsic line shape fitted to narrow peaks. The broad states in ^{9}Be constitute a complicated background under the ^{16}O peaks of current interest. These were also treated as Lorentzians convoluted with the shape appropriate to narrow states of ^{9}Be. We found it necessary to vary the position and width of the strong broad state listed in the compilation of Ref. 9 as 6.76 MeV with a nominal width of 1.54 MeV. Further details of the analysis of the ^{9}Be spectrum can be found in Ref. 10.

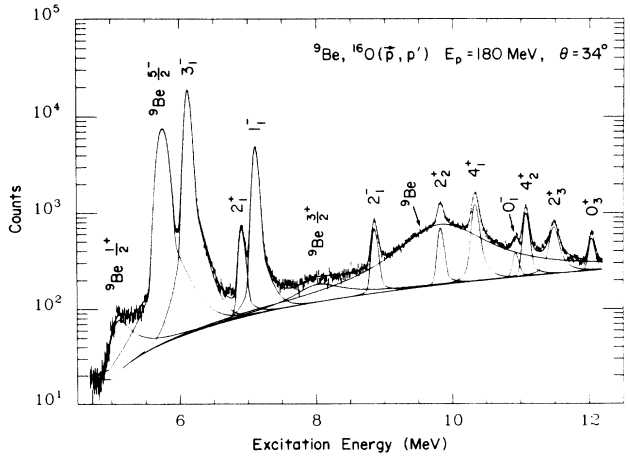

FIG. 1. Sample spectrum for the 5.5–12.5-MeV excitation region of ^{16}O obtained by scattering 180 MeV protons through 34° using a BeO target.

Data tables are on deposit with the Physics Auxiliary Publication Service (PAPS).[11] Normal-parity data include elastic scattering and the 0_2^+ (6.049 MeV), 0_3^+ (12.049 MeV), 1_1^- (7.117 MeV), 2_1^+ (6.917 MeV), 2_2^+ (9.847 MeV), 2_3^+ (11.521 MeV), 3_1^- (6.130 MeV), and 4_1^+ (10.353 MeV) states. In addition, data for the 0_1^- (10.952 MeV) and 2_1^- (8.872 MeV) abnormal-parity transitions and for an unresolved $(4_2^+, 3_1^+)$ doublet at 11.09 MeV are also tabulated. The data for most states extend to momentum transfers of about 3.2 fm^{-1}. Data for elastic scattering and for a few of the isolated peaks were extended to nearly 4.0 fm^{-1} using the thickest target.

III. REACTION MODEL

Calculations were performed using the procedures described in detail in Refs. 1 and 2. For the present purposes it suffices to summarize the salient features.

Proton transition densities extracted from the electroexcitation measurements of Buti *et al.*,[8] corrected for the nucleon form factor, were used to specify the nuclear structure. The ground-state density was obtained from Ref. 12. Charge symmetry is invoked to equate neutron and proton transition densities. We assume that all spin and current densities are negligible because the transverse electromagnetic form factors were found to be very small for all normal-parity transitions considered herein. Therefore, proton scattering data can be used to study the two-nucleon effective interaction with little uncertainty due to nuclear structure.

Scattering calculations were performed using a form of the local density approximation (LDA) in which the density dependence of the effective interaction is evaluated at the site of the projectile.[2] Exchange is included in zero-range approximation. Optical potentials were computed from the same effective interactions assumed to drive the inelastic transitions. Rearrangement contributions to inelastic scattering are included by applying the Cheon factor $(1 + \rho\partial/\partial\rho)$ to the elastic interaction.[13]

Three nuclear matter calculations have been performed for the effective interaction in this energy regime. First, Brieva, Rook, and von Geramb (BRG) constructed a positive-energy G matrix using the Hamada-Johnston potential.[3] Later, von Geramb and his Hamburg collaborators used the Paris potential to produce a more refined interaction designated as PH.[4] Finally, Nakayama and Love (NL) constructed an effective interaction based upon the Bonn potential.[5] However, these three calculations used different approximations and different prescriptions for distilling local pseudopotentials from

TABLE I. Reparametrization of 180 MeV G matrices.

Component	Coefficient	μ[a]	PH	NL	BRG
$\mathrm{Re}t_{00}^{C}$	a_1(MeV fm^3)	0	−74.33	0.34	15.00
	a_2(MeV fm^3)	3.0 fm^{-1}	157.32	24.93	161.43
$\mathrm{Im}t_{00}^{C}$	a_0		0.326	0.568	0.608
	a_1(MeV fm^3)	0	−10.27	−4.96	−21.82
$\mathrm{Re}\tau_0^{LS}$	a_1(MeV fm^5)	3.0 fm^{-1}	−8.73	−14.14	−7.96
	a_2(MeV fm^5)	6.0 fm^{-1}	7.21	9.18	5.96
$\mathrm{Im}\tau_0^{LS}$	a_0		0.586	0.663	0.677
	a_1(MeV fm^5)	3.0 fm^{-1}	−5.64	−1.30	−4.45

[a]An entry of 0 is to be interpreted as a delta function with $\mu^{-1}=0$.

their nuclear matter results. Therefore, the rather large differences between their effective interactions probably reflect differences in strategy rather than differences in basic nucleon-nucleon potentials.[2]

Medium modifications to the effective interaction are most conveniently represented by the parametrization[1]

$$t_i(q,\kappa_F)=(S-a_0\kappa_F^{\gamma_0})t_i(q,0)$$
$$+\kappa_F^{\gamma_1}q^{\delta}\sum_{n=1}^{N}a_n\left[1+\left[\frac{q}{\mu_n}\right]^2\right]^{-\beta}, \quad (1)$$

where $\kappa_F=k_F/1.33$ describes the local Fermi momentum relative to saturation and where the index i distinguishes various components of the t matrix. The exponent β assumes the values 1 for central, 2 for spin-orbit, and 3 for tensor interactions. Similarly, we use $\delta=2$ for tensor interactions and $\delta=0$ otherwise. These functions can be used to reparametrize theoretical interactions by requiring the scale factor S to be unity, so that the free interaction is recovered at zero density; this restriction can be relaxed for phenomenological analyses. Good fits to any of the G matrices available from nuclear matter calculations are obtained using $\gamma_0=\gamma_1=3$ for real parts and $\gamma_0=\gamma_1=2$ for imaginary parts of both central and spin-orbit interactions. The free interactions $t_i(q,0)$ are obtained by extrapolating the appropriate G matrix to zero density. Parameters fitted to the PH, NL, and BRG interactions are compared in Table I. The accuracy with which these parametrizations reproduce the original calculations is comparable to the corresponding figures shown in Ref. 1 for 135 MeV.

Data analysis is performed using the somewhat simpler parametrization[1]

$$\mathrm{Re}t_{00}^{C}(q,\kappa_F)=S_1\,\mathrm{Re}t_{00}^{C}(q,0)+\kappa_F^3 b_1\left[1+\left[\frac{q}{\mu_1}\right]^2\right]^{-1}, \quad (2a)$$

$$\mathrm{Im}t_{00}^{C}(q,\kappa_F)=(S_2-b_2\kappa_F^2)\,\mathrm{Im}t_{00}^{C}(q,0), \quad (2b)$$

$$\mathrm{Re}\tau_0^{LS}(q,\kappa_F)=S_3\,\mathrm{Re}\tau_0^{LS}(q,0)+\kappa_F^3 b_3\left[1+\left[\frac{q}{\mu_3}\right]^2\right]^{-2}, \quad (2c)$$

designed to minimize correlations among parameters fitted to scattering data. The choices $\mu_1=1.5$ fm^{-1} and $\mu_3=6.0$ fm^{-1} provide fits to theoretical interactions that are almost as good as those based upon Eq. (1). Estimates for the b_i parameters, obtained by fitting the PH interaction for $0\le q\le 3$ fm^{-1} subject to $S_i=1$, are listed in Table II. The b_1 parameter, describing a repulsive core in $\mathrm{Re}t_{00}^{C}$ that is proportional to density, is predicted to be almost constant between 135 and 180 MeV. The b_2 parameter, describing Pauli blocking of $\mathrm{Im}t_{00}^{C}$ that is linear in κ_F^2, is predicted to show an energy dependence similar to the E^{-1} behavior of the Clementel and Villi model.[14] The b_3 parameter, describing the density dependence of $\mathrm{Re}\tau^{LS}$, is predicted to be small and nearly independent of energy. The contributions of $\mathrm{Im}\tau^{LS}$ are so small that this term was taken from the PH theory and held fixed.

TABLE II. Effective interactions at 135 and 180 MeV.

E_p	Interaction	S_1[a]	b_1	S_2	b_2	S_3	b_3
135	PH	[1.0]	90.0	[1.0]	0.415	[1.0]	2.57
	Empirical[b]	0.839	56.8	0.812	0.435	0.840	3.14
180	PH	[1.0]	89.4	[1.0]	0.272	[1.0]	2.11
	Empirical	0.749	62.9	0.764	0.228	0.883	0.51

[a]Square brackets indicate fixed parameter.
[b]Reference 1.

IV. RESULTS

A. Empirical effective interaction

The principal results of this investigation are displayed in Figs. 2 and 3. LDA calculations based upon the Paris-Hamburg G-matrix are presented as dashed curves and impulse approximation (IA) calculations based upon its zero-density limit are presented as dotted curves, both using LDA optical potentials. Strong density-dependent corrections to transitions with interior densities, such as the 0_3^+ and 1_1^- states, are observed. The 1^- cross section, for example, is strongly suppressed for $q < 1.2$ fm^{-1} and strongly enhanced for $q > 1.5$ fm^{-1} by Pauli blocking corrections. Similarly, the analyzing power angular distributions are also strongly affected. The changes in the 0_3^+ analyzing power are especially dramatic. The PH interaction describes these effects qualitatively well, especially for the interior transitions. However, surface states such as the 2_1^+, 3_1^-, and 4_1^+ seem to require considerably stronger medium modifications than predicted by the PH interaction. Although calculations using other interactions at 180 MeV are not displayed here, we note that the PH description of both elastic scattering and normal-parity transitions is much superior to either BRG or NL interactions as also found at 135 MeV.[2]

An empirical effective interaction, producing the solid curves in Figs. 2 and 3, was fitted to these data using the parametrization and procedures of Ref. 1. Specifically, the PH interaction was used to produce optical potentials for the first iteration in which six parameters of the effective interaction were fitted to cross section and analyzing power data for five inelastic transitions simultaneously (1_1^-, 2_1^+, 2_3^+, 3_1^-, and 4_1^+). Fitted interactions were then used to generate self-consistent distorting potentials for subsequent iterations. To improve the stability of this procedure, we use the average of the previous two fits to produce the optical potential for the next iteration. About five iterations were needed to reach convergence.

For most states, electron scattering data are available only for $q < 2.7$ fm^{-1}. Hence, the form factors for larger momentum transfer are poorly constrained and may contain unrealistic oscillations. Thus, the rapid oscillations present in the calculations for large momentum transfer cannot be taken too seriously. Moreover, several aspects of the reaction model can also be expected to fail for larger momentum transfer. Therefore, the fits are limited to data with $q \leq 2.7$ fm^{-1}. Nevertheless, our figures include the entire range of momentum transfer spanned by the experiment.

The quality of these results is quite impressive for a fit to cross section and analyzing power angular distributions for six states simultaneously, using only six free pa-

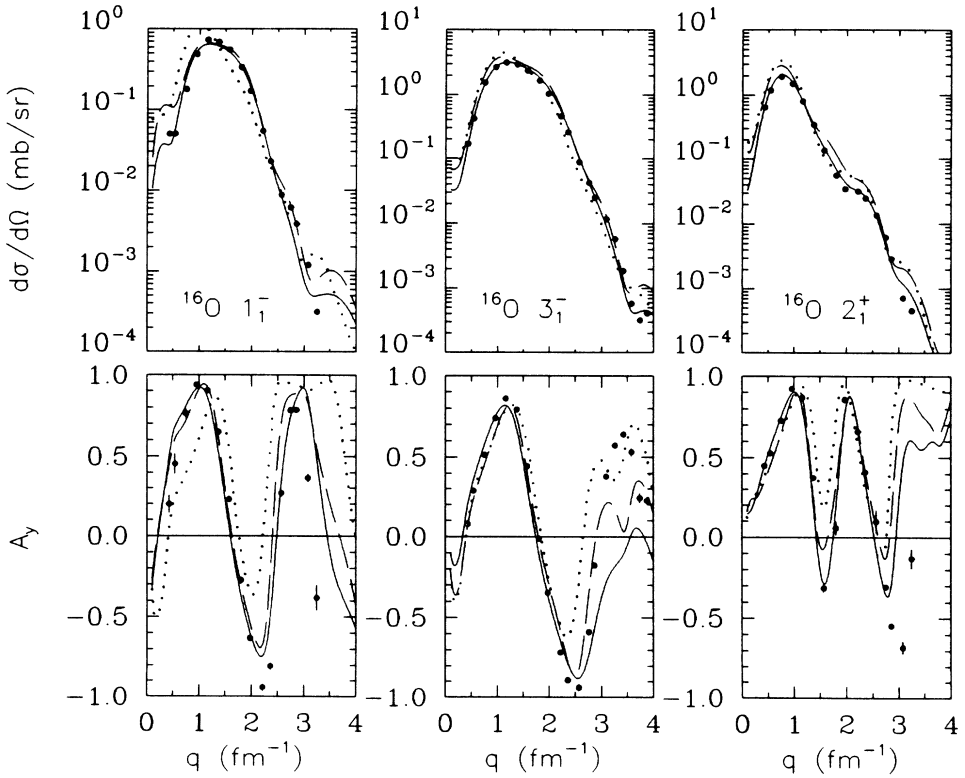

FIG. 2. Fits to the 180-MeV data for the 1_1^-, 3_1^-, and 2_1^+ states of ^{16}O are shown as solid curves. Note that only the data for $q \leq 2.7$ fm^{-1} were fitted. For comparison, IA calculations are shown as dotted curves and PH calculations as dashed curves.

rameters. Equally impressive are the elastic scattering predictions, shown in Fig. 4, obtained without including these data in the analysis. Both elastic and inelastic calculations benefit from self-consistent iteration of the distorting potential. Similar results have also been obtained for ^{28}Si.[6,15] Therefore, we conclude that the effective interaction for 180 MeV nucleons depends strongly upon local density but is independent of final state. This result also supports the accuracy of the rearrangement factor[13] $(1+\rho\partial/\partial\rho)$ which relates the density dependence of elastic and inelastic interactions.

Except for cross section in the range $1<q<2$ fm^{-1}, the empirical interaction fits the 0_3^+ data very well, whether or not these data are included in the search procedure. The analyzing power for $q<1.5$ fm^{-1} is particularly impressive. However, the calculations substantially underestimate the cross section in the vicinity of 1.5 fm^{-1}, near this state's form factor minimum. This effect is somewhat smaller at 180 MeV than at 135 MeV and is probably due to a spin-convection density that is not included in these calculations.[2] This density would have only small effects upon electron scattering, but may contribute to the ^{16}O$(p,p')0_3^+$ cross section near 1.5 fm^{-1}.[16]

Medium modifications cause larger effects at 135 MeV, but remain quite important at 180 MeV also. Similarly, the differences between calculations based upon the PH and empirical interactions are somewhat smaller at 180 MeV. However, although the PH interaction provides the best theoretical description of these data available, systematic deficiencies in the LDA description of surface states are observed. The differences between IA and LDA calculations for 3_1^-, 2_1^+, and 4_1^+ states are too large to correct without invoking modifications of the interaction at zero density. Of the three scale factors, only S_2 can be constrained to unity without seriously compromising the quality of the fit. For the best results we find that both the real and imaginary parts of the central interaction require scale factors of about 0.75 at zero density, which can be compared to about 0.82 for 135 MeV. The inelastic data cannot be fitted, nor can self-consistency between elastic and inelastic scattering be achieved, with unit scale factors.

We have also performed fits using several variations of the fitting function. For example, the Franey-Love interaction[17] can be used to describe $t(q,0)$ in place of the PH interaction at zero-density. Although the fitted parameters change slightly, the interaction itself hardly changes. Similarly, the essential characteristics of the empirical effective interaction are insensitive to the set of states analyzed or to the relative weights assigned to the data. Finally, essentially the same results have been obtained for ^{28}Si. Therefore, we consider the basic characteristics of the effective interaction to be unambiguously determined by this analysis.

The parameters of the empirical effective interaction for 180 MeV protons are compared in Table II with the

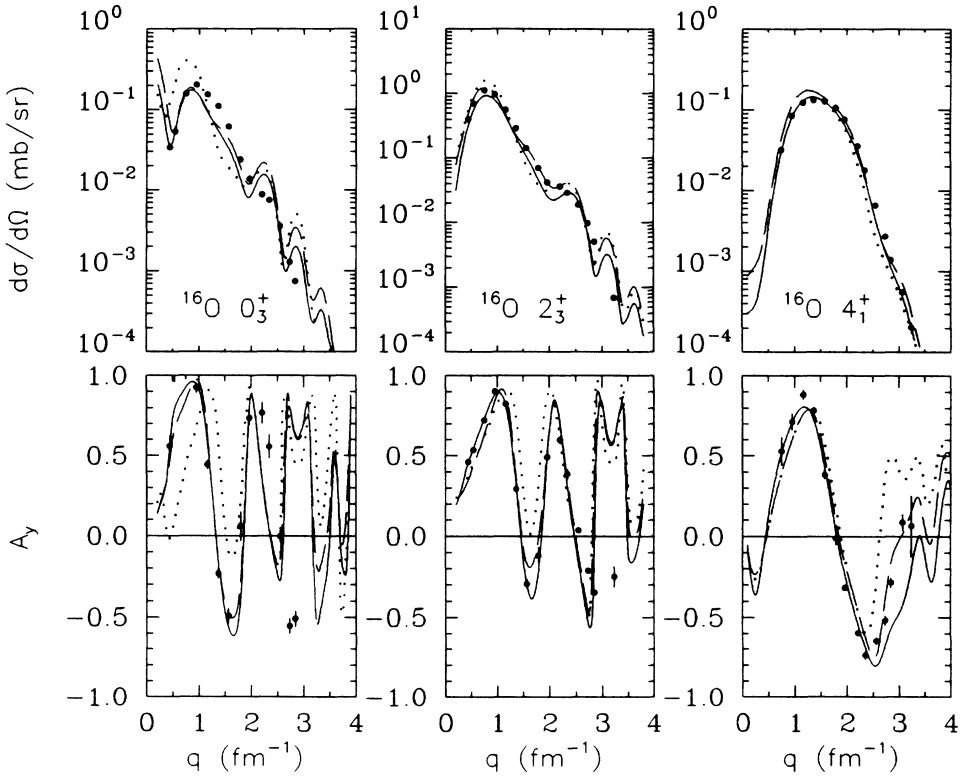

FIG. 3. Fits to the 180-MeV data for the 0_3^+, 2_3^+, and 4_1^+ states of ^{16}O are shown as solid curves. Note that only the data for $q\leq 2.7$ fm^{-1} were fitted. For comparison, IA calculations are shown as dotted curves and PH calculations as dashed curves.

corresponding results for 135 MeV. The repulsive core in $\mathrm{Re}t_{00}^{C}$ seems to be slightly stronger at 180 than at 135 MeV. On the other hand, the Pauli blocking factor b_2 seems to be roughly consistent with the E^{-1} behavior predicted by the phase-space model of Clementel and Villi.[14] The scale factors that must be applied to the central interaction are even smaller at 180 than at 135 MeV. Finally, the density dependence of $\mathrm{Re}t^{LS}$ is small at both energies.

These results should also be compared with the theoretical parameters listed in Tables I and II. The fitted interaction is compared in Fig. 5 with the PH theory for $k_F=0.0$, 0.6, 1.0, and 1.4 fm^{-1}, corresponding to zero density and about a tenth, a half, and full saturation density. Although similar in form to the PH interaction, substantial changes in the interaction are required to fit inelastic and elastic scattering data self-consistently. Pauli blocking in finite nuclei appears to be more effective at low density than predicted for infinite nuclear matter. The suppression of the spin-orbit interaction is also quite significant.

B. Other normal-parity transitions

Similar calculations for the 0_2^+, 2_2^+, and 4_2^+ states, which were omitted from the fitting procedure, are compared with data in Fig. 6. Density dependent corrections to the 0_2^+ transition appear to be quite important, but the data are rather sparse because this state is separated from the much stronger 3^- state by only 80 keV. However, although the analyzing power is described very well when density dependence is included, both the PH and the empirical effective interaction substantially underestimate the cross section for this state.

The calculations for the 2_2^+ state, on the other hand, are somewhat less successful than for most other states. However, we have previously argued that the 135-MeV data for the 2_2^+ state show evidence for multistep excitation.[2] This argument is based on the fact that the $2_1^+ \rightarrow 2_2^+$ branch possesses an electromagnetic matrix element that is much stronger than the direct matrix element and hence may make an important contribution to proton scattering. At 135 MeV, the 2_2^+ cross section observed near the peak of the 2_1^+ form factor is substantially larger than predicted for direct excitation by the PH interaction. More importantly, the analyzing power ob-

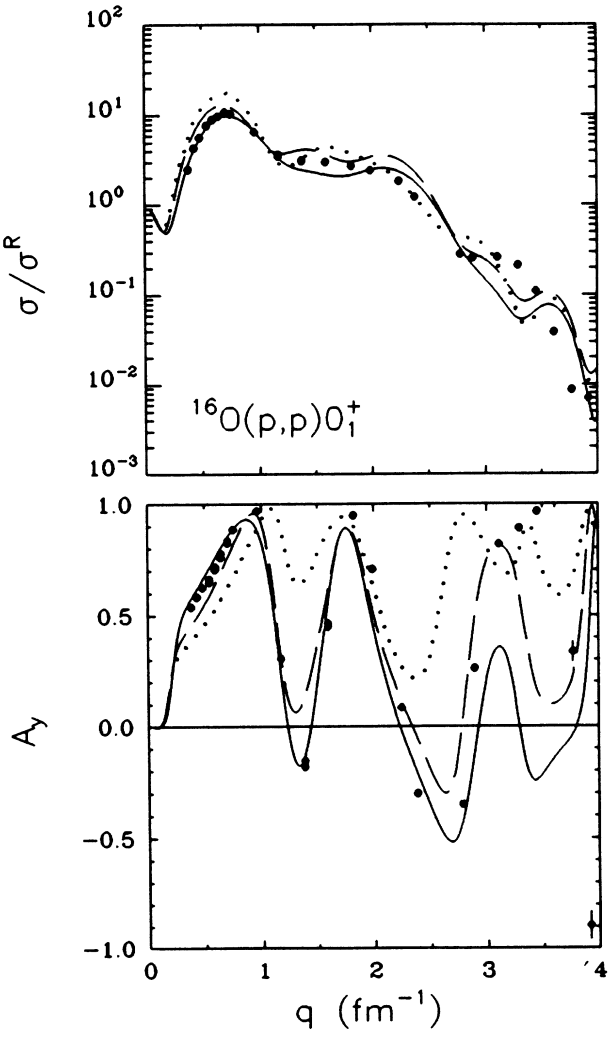

FIG. 4. Elastic scattering data are compared with calculations based upon the empirical effective interaction (solid curves), free interaction (dots), and PH interaction (dashes). Elastic cross sections are presented as ratios to Rutherford (σ_R) to enhance detail.

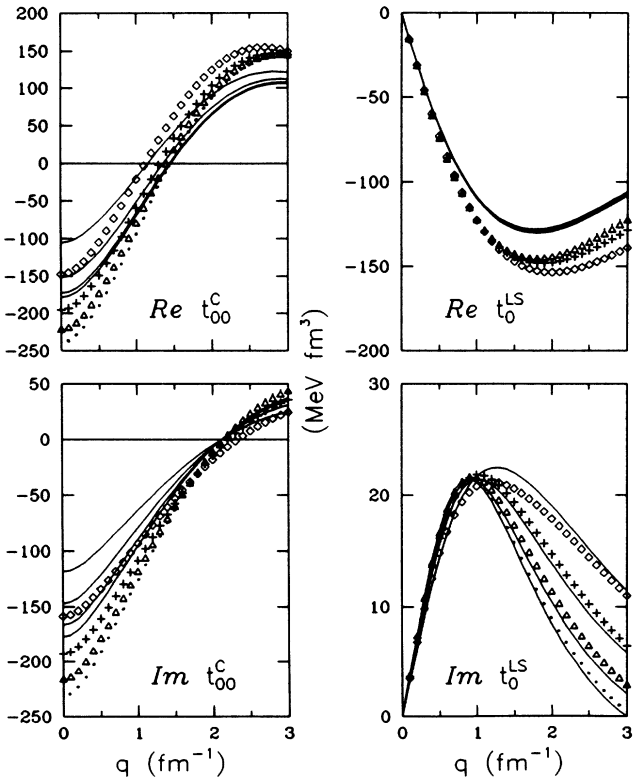

FIG. 5. The empirical effective interaction (solid curves) is compared with PH calculations for $k_F=0.0$ fm^{-1} (dots), 0.6 fm^{-1} (triangles), 1.0 fm^{-1} (plus signs), and 1.4 fm^{-1} (diamonds). The units are MeV fm^3.

served in this region is also much smaller than predicted and has a shape uncharacteristic of strong normal-parity excitations. These effects suggest an indirect contribution for $q < 2$ fm^{-1}. Although the direct calculations for the 180-MeV cross section, shown in Fig. 6, are more successful, the analyzing power data still exhibit the same signature of multistep excitation. Therefore, it appears that the relative importance of multistep processes decreases slowly between 135 and 180 MeV.

Finally, we observe that at large momentum transfer the 4_2^+ cross section is substantially larger than we predict and that its analyzing power is anomalously small. However, this state cannot be resolved from an adjacent 3^+ state. Because abnormal-parity transitions generally have small analyzing powers, an unresolved contribution of this type can be expected to enhance the cross section and reduce the analyzing power attributed to the dominant normal-parity state. Therefore, we can probably attribute the large-q deviation between data and calculations to an unresolved state.

Given that LDA calculations based upon electroexcitation form factors and the empirical effective interaction accurately describe most normal-parity transitions, unusual deviations require unusual explanations. In the present case we attribute the bulge in the 0_3^+ cross section to a spin-convection density, and the enhanced cross sections and uncharacteristic analyzing powers of the 2_2^+ and 4_2^+ states to multistep or unresolved contributions, respectively. Inferences of this kind should now be taken more seriously than could be justified for earlier models.

C. Abnormal-parity transitions

Calculations for abnormal-parity transitions require considerably more nuclear structure information than can be extracted directly from electroexcitation measurements. Moreover, proton scattering proceeds through three interaction components: spin-dependent central, spin-orbit, and tensor. Therefore, it does not seem possible to extend our analysis of the effective interaction to abnormal-parity transitions without considerable ambiguity. Nevertheless, in this section we compare data for the isoscalar 0_1^- and 2_1^- states with representative calculations.

The calculations shown in this section employ oscillator wave functions with $b = 1.77$ fm^{-1}, including a center-of-mass form factor. The PH interaction is used for both distorting and transition potentials. Although not necessarily well justified for abnormal-parity transitions, the $(1+\rho\partial/\partial\rho)$ rearrangement factor is included in the transition potential. Calculations are compared for the present 180-MeV data and for the 135-MeV data of Ref. 2.

In Fig. 7 we compare data for the 0_1^- state of ^{16}O with calculations based upon the simplest possible configuration, namely, $(2s_{1/2}, 1p_{1/2}^{-1})$. Except for a deep minimum calculated for momentum transfers near 1.2 fm^{-1}, the cross-section data are well described by a spectroscopic amplitude of 0.7. The data for both energies seem to require an additional contribution to fill the deep minimum in the calculated cross section. Small but nonvanishing analyzing powers are also observed; direct exci-

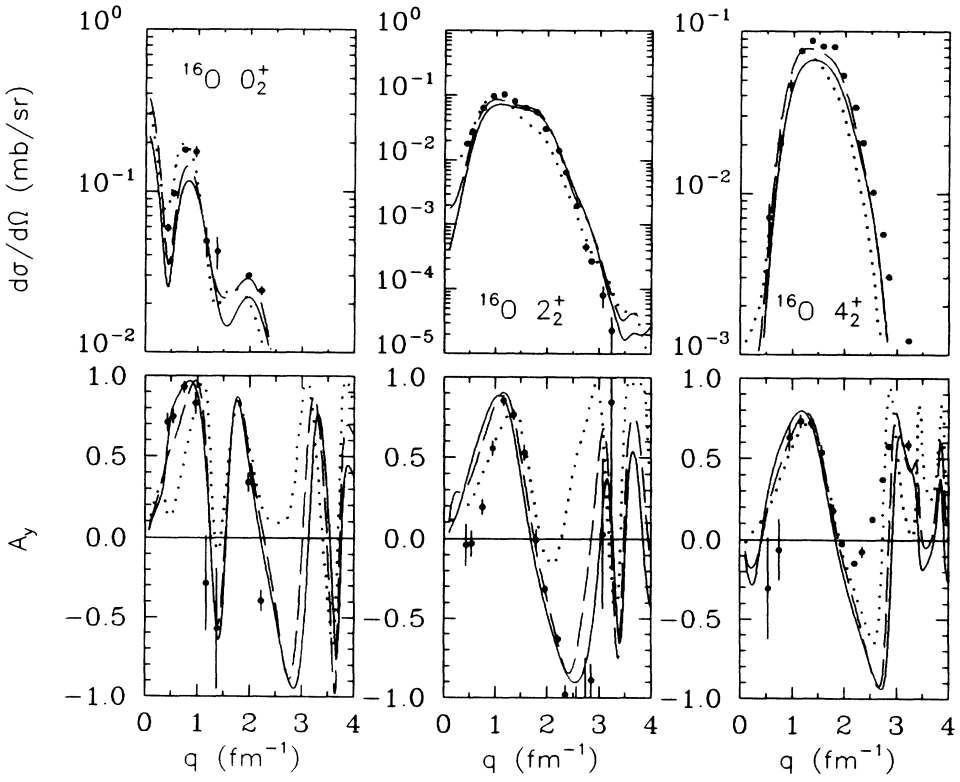

FIG. 6. Data for the 0_2^+, 2_2^+, and 4_2^+ states of ^{16}O are compared with calculations based upon the empirical effective interaction (solid curves). In addition, IA calculations are shown as dotted curves and PH calculations as dashed curves.

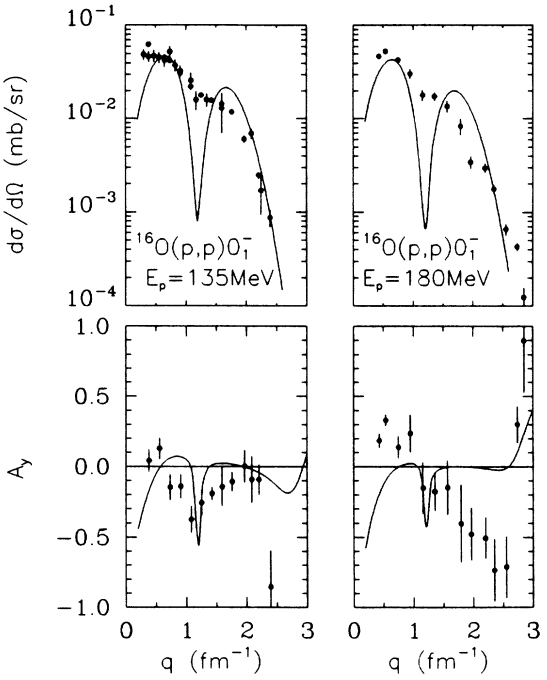

FIG. 7. Data for the excitation of the 0_1^- state of ^{16}O by 135 and 180 MeV protons are compared with calculations based upon the $(2s_{1/2}, 1p_{1/2}^{-1})$ configuration with spectroscopic amplitude 0.7. The PH interaction was used with the rearrangement factor included.

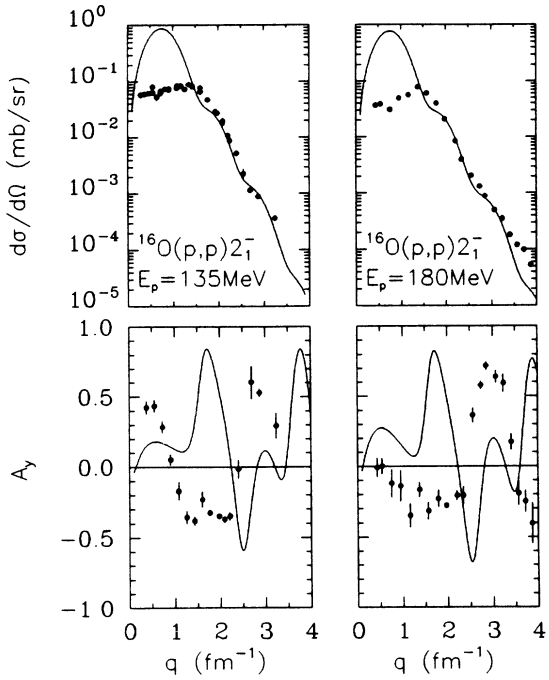

FIG. 8. Data for the excitation of the 2_1^- state of ^{16}O by 135 and 180 MeV protons are compared with calculations based upon a $1\hbar\omega$ wave function. The PH interaction was used with the rearrangement factor included.

tation via a purely local interaction would produce vanishing analyzing power for $0^+ \rightarrow 0^-$ transitions.[18]

A $1\hbar\omega$ wave function provided by Millener[19] was used to produce the calculations shown in Fig. 8 for the 2_1^- state. The spectroscopic amplitudes are listed in Table III. In addition, we compare the calculated transverse form factor with the electron scattering data of Ref. 20 in Fig. 9. We find that this wave function describes the (e,e') data fairly well, but the (p,p') cross section calculated for $q < 1.5$ fm^{-1} is about an order of magnitude too large. Use of the NL interaction or elimination of the rearrangement factor do not improve this situation significantly. Nor do modest variations of the $1\hbar\omega$ wave function help. Although two-step excitation via the giant octupole resonance has been studied for $E_p = 23$–46 MeV,[21] this contribution decreases with higher energy and is never large enough to account for the differences shown in Fig. 8. We do not expect this mechanism to become crucial for $E_p = 135$–180 MeV.

Apparently, the electron and proton scattering data are sensitive to different aspects of the wave function. The calculated transverse form factor is about a factor of 2 too small for $q < 1.5$ fm^{-1}. Perhaps an additional component in the wave function could produce mild constructive interference for (e,e') and strong destructive interference for (p,p') for similar momentum transfers. If we had confidence in the accuracy of the relevant components of the two-nucleon effective interaction, a combined analysis of electron and proton scattering data could reveal much about the wave function. The significant energy dependence shown by the (p,p') cross section should also help. However, a thorough analysis of this kind is beyond the scope of the present work.

V. CONCLUSIONS

The two-nucleon effective interaction for $E_p = 100$–200 MeV is strongly affected by the local density in the interaction region. Pauli blocking is an important source of density dependence that is amenable to nuclear matter theory. However, substantial ambiguities plague *ab initio* calculations of the effective interaction. Although the density dependencies that emerge from the three avail-

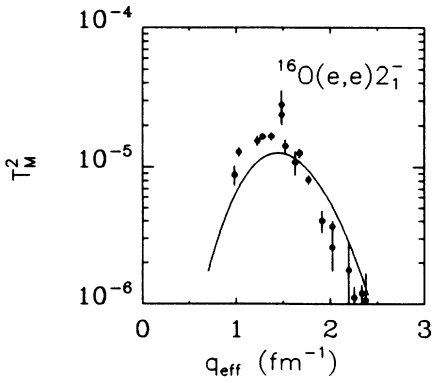

FIG. 9. The transverse magnetic form factor is compared with electron scattering data for the 2_1^- state of ^{16}O.

TABLE III. Spectroscopic amplitudes for 0_1^- and 2_1^- states of ^{16}O.

State	Amplitudes[a] $1d_{5/2}1p_{1/2}^{-1}$	$1d_{5/2}1p_{3/2}^{-1}$	$2s_{1/2}1p_{1/2}^{-1}$	$2s_{1/2}1p_{3/2}^{-1}$	$1d_{3/2}1p_{1/2}^{-1}$	$1d_{3/2}1p_{3/2}^{-1}$
0_1^- [b]			0.7			
2_1^- [c]	−0.8704	−0.3217	0	−0.0540	−0.3673	0.0316

[a]Amplitudes $Zf^i(\alpha,\beta)=\langle f\|\|[a_\alpha^+\otimes a_\beta]_J\|\|i\rangle$ using Brink-Satchler (Ref. 22) reduced matrix elements and real orbitals.
[b]Adjusted to describe (p,p') data.
[c]Supplied by Millener (Ref. 19).

able calculations are similar in form, the quantitative differences are quite large. Faced with these difficulties, it is almost impossible to assess the applicability of the local density approximation using the theoretical calculations that are presently feasible.

Therefore, it is necessary to develop a phenomenology guided by the essential characteristics of the nuclear matter results. Transition densities determined from electron scattering measurements are used to minimize uncertainties due to nuclear structure. The parameters of an empirical effective interaction are then fitted to inelastic scattering data for many states simultaneoulsy, using self-consistent distorting potentials. For the LDA to be considered sound, we ask that the empirical effective interaction satisfy three primary criteria. First, a unique interaction should be able to fit all relevant data for a given target and energy simultaneously. Second, the interaction should also be independent of target. Third, the parameters should depend smoothly upon energy in a manner consistent with theoretical expectations. In this paper we have tested the first and third criteria.

We have shown that a unique empirical effective interaction provides an excellent simultaneous fit to data for many states of ^{16}O excited by 180 MeV protons. The same effective interaction also describes elastic scattering and distortion self-consistently. Therefore, the effective interaction depends strongly upon density but appears to be independent of state. Furthermore, the parameters are similar to those found at 135 MeV. The energy dependence of the Pauli blocking parameter is consistent with E^{-1} behavior predicted by the simple Clementel-Villi phase-space model and by more sophisticated nuclear matter calculations.

Although qualitatively similar to theoretical interactions, the empirical interaction differs in two important respects. First, the low-density limit is suppressed with respect to the free interaction— the effective interaction for finite nuclei never heals to the free interaction because target nucleons are nowhere free. Second, the subsequent density dependence of the empirical interaction is substantially smaller than predicted by nuclear matter calculations. These properties of the empirical interaction are essentially independent of the details of the parametrization and the analysis and agree with earlier observations at 135 MeV. These results suggest nonlocal density dependence in finite nuclei. Evidently, Pauli blocking in finite nuclei is more effective in the tail regions and less effective in the interior than expected for infinite nuclear matter of corresponding density. Nevertheless, the consistency of the empirical interaction suggests that a local approximation to the G matrix for finite nuclei is still possible.

ACKNOWLEDGMENTS

We thank Dr. D.J. Millener for shell model calculations. This work was supported by the National Science Foundation and the U.S. Department of Energy.

[1]J. J. Kelly, Phys. Rev. C **39**, 2120 (1989).
[2]J. J. Kelly, W. Bertozzi, T. N. Buti, J. M. Finn, F. W. Hersman, C. Hyde-Wright, M. V. Hynes, M. A. Kovash, B. Murdock, B. E. Norum, B. Pugh, F. N. Rad, A. D. Bacher, G. T. Emery, C. C. Foster, W. P. Jones, D. W. Miller, B. L. Berman, W. G. Love, J. A. Carr, and F. Petrovich, Phys. Rev. C **39**, 1222 (1989).
[3]F. A. Brieva and J. R. Rook, Nucl. Phys. **A291**, 299, 317 (1977); **A297**, 206 (1978); **A307**, 493 (1978); H. V. von Geramb, F. A. Brieva, and J. R. Rook, in *Microscopic Optical Potentials*, edited by H. V. von Geramb (Springer, Berlin, 1979), p. 104.
[4]H. V. von Geramb, in *The Interaction Between Medium Energy Nucleons in Nuclei—1982*, edited by H. O. Meyer (AIP Conf. Proc. No. 97) (AIP, New York, 1983), p. 44; L. Rikus, K. Nakano, and H. V. von Geramb, Nucl. Phys. **A414**, 413 (1984).
[5]K. Nakayama and W. G. Love, Phys. Rev. C **38**, 51 (1988).
[6]Q. Chen, J. J. Kelly, P. P. Singh, M. C. Radhakrishna, W. P. Jones and H. Nann, Phys. Rev. C **41**, 2514 (1990).
[7]J. J. Kelly, Q. Chen, P. P. Singh, M. C. Radhakrishna, W. P. Jones, and H. Nann, Phys. Rev. C **41**, 2525 (1990).
[8]T. N. Buti, J. Kelly, W. Bertozzi, J. M. Finn, F. W. Hersman, C. Hyde-Wright, M. V. Hynes, M. A. Kovash, S. Kowlaski, R. W. Lourie, B. Murdock, B. E. Norum, B. Pugh, C. P. Sargent, W. Turchinetz, and B. L. Berman, Phys. Rev. C **33**, 755 (1986).
[9]F. Ajzenberg-Selove, Nucl. Phys. **A490**, 1 (1988).
[10]S. Dixit, Master's thesis, MIT, 1986.
[11]See AIP document no. PAPS PRVCA-41-2504-13 for 13 pages containing a complete tabulation of the data described in this paper. Order by PAPS number and journal reference from American Institute of Physics, Physics Auxiliary Publication Service, 335 E. 45th Street, New York, NY 10017. The price is $1.50 for each microfiche or $5.00 for photocopies. Air mail additional. Make checks payable to the American Institute of Physics.
[12]H. de Vries, C. W. de Jager, and C. de Vries, At. Data Nucl.

Data Tables **36**, 495 (1987).
[13]T. Cheon, K. Takayanagi, and K. Yazaki, Nucl. Phys. **A437**, 301 (1985); **A445**, 227 (1985); T. Cheon and K. Takayanagi, *ibid.* **A455**, 653 (1986).
[14]E. Clementel and C. Villi, Nuovo Cimento **2**, 176 (1955).
[15]Q. Chen, P. P. Singh, M. C. Radhakrishna, W. P. Jones, H. Nann, and J. J. Kelly, Bull. Am. Phys. Soc. **33**, 962 (1988); Q. Chen, Ph.D. thesis, Indiana University, 1989.
[16]F. Petrovich, J. A. Carr, R. J. Philpott, A. W. Carpenter, and J. Kelly, Phys. Lett. **165B**, 19 (1985).
[17]M. A. Franey and W. G. Love, Phys. Rev. C **31**, 488 (1985).
[18]S. S. M. Wong, R. E. Azuma, T. E. Drake, J. D. King, and X. Zhu, Phys. Lett. **149B**, 299 (1984).
[19]D. J. Millener, private communication.
[20]C. Hyde-Wright, Ph.D. thesis, MIT, 1984.
[21]H. V. Geramb, R. Sprickmann, and G. L. Strobel, Nucl. Phys. **A199**, 545 (1973); R. Smith and K. Amos, Phys. Lett. **55B**, 162 (1975).
[22]D. M. Brink and G. R. Satchler, *Angular Momentum* (Oxford University Press, London, 1968).